

The study of velocity field of the dynamical air flow developing around the spatial structure of a petroleum coke plant using the F.E.M.

Mihai D.L. Țălu, Ștefan D.L. Țălu and Marin Bică

Abstract— This paper presents a part of results concerning the simulation of the aerodynamics flow velocity field developing surround a petrochemistry petroleum coke plant. The spatial distributions of velocity is result as impact between the air and the spatial structure of plant. The punctual values of velocity are determinated through numerical simulations using the F.E.M. which have initial data determinated through experimental measurements. After this calculus the theoretical results are compared with the real measurements make in few important points and calculated the corresponding errors. The Cosmos Flow 2007 software was used to make the analysis through numerical simulation. The obtained results confirm the accuracy of method and assure the possibility to use this method with confidence in activity of design process of a petroleum coke plant.

Keywords - Finite element method (F.E.M.), petroleum coke plant, numerical simulation, velocity field.

I. INTRODUCTION

IN Romania the production of petroleum coke in majority of cases is based on the method of tardy carbon – producing. This study developed in this paper is concentrated on investigation of the velocity field developed around a petrochemistry petroleum coke plant which working at 1996 on the Onesti oil distillery platform.

The real installation is an ensemble constituted with four identical section presented in Fig. 1 and which alternatively work in cycles by 48 hours in according with the algorithm of the technological process, [17].

Manuscript received September 7, 2008; Revised received November 18, 2008. This work was supported in part by the Romanian Ministry of Education, Research and Youth, through The National University Research Council, Grant PN-II-ID-PCE-2007-1, no. 440/1.10.2007, code ID_1107, 2007 - 2010.

Mihai D.L. Țălu is with the University of Craiova, Romania. He is now with the Department of Applied Mechanics, Faculty of Mechanics, 165 Calea Bucuresti Street, Craiova, 200585 Romania (phone: +40-251-418-803; fax: +40-251-418-803; e-mail: mihai_talu@yahoo.com).

Ștefan D.L. Țălu is with the Technical University of Cluj-Napoca, Romania. He is now with the Department of Descriptive Geometry and Engineering Graphics, Faculty of Mechanics, 103-105 B-dul Muncii Street, Cluj-Napoca, 400641 Romania (e-mail: stefan_ta@yahoo.com).

Marin Bică is with the University of Craiova, Romania. He is now with the Department of Road Vehicles, Faculty of Mechanics, 165 Calea Bucuresti Street, Craiova, 200585 Romania (phone: +40-251-418-803; fax: +40-251-418-803; e-mail: mbica@mecanica.ucv.ro).

The solicitation of wind represents an important loading which must obligatory to take into consideration in design activity of plant.

For this reason is demanding to make a detailed investigation of velocity field which is straight lied with other sizes as pressure, viscosity and density as it show in the Navier-Stokes equation used to describe the dynamical flow of the real fluids [15] and [16].

II. THE SPATIAL MODEL OF THE PETROLEUM COKE PLANT

The spatial model of plant is made with aid of the SolidWorks 2007 softwear [24] starting at the original execution drawings of the installation.

The dimensional sizes of plant are big $28 \times 6 \times 6 \text{ m}^3$ and the geometry is complicated, Fig. 1. Also the spatial model was presented in papers [17] to [21].

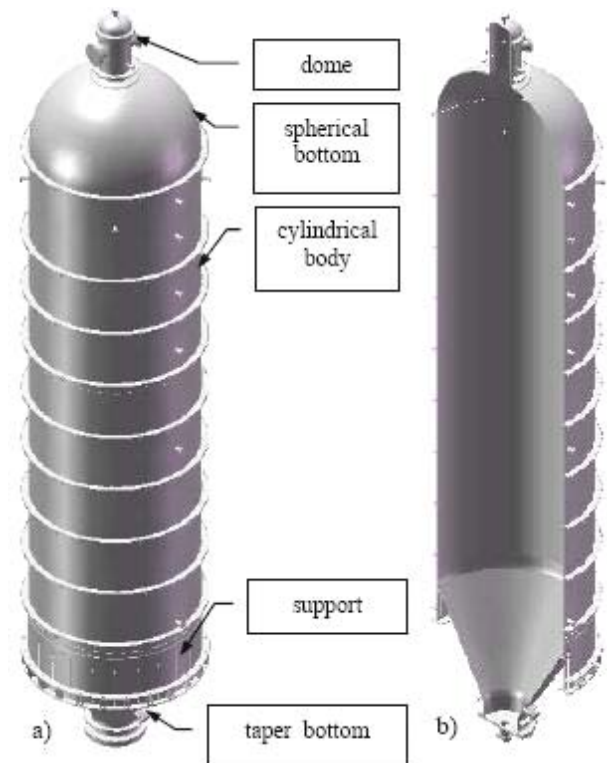


Fig. 1. The spatial model of the petroleum coke plant

In Fig. 1 is given the 3D isometric view with no a) and with section b) where is mark the important elements of plant.

In Fig. 2 and in Fig. 3 are presented the 3D isometric view with section of the ensembles dome - spherical bottom and taper bottom - support of plant.



Fig. 2. The spatial section through the spherical bottom - dome



Fig. 3. The spatial model of the ensemble taper bottom - support

The 3D isometric model of the petroleum coke plant view from the direction taper bottom to dome is given in Fig. 4.



Fig. 4. The 3D isometric model of the petroleum coke plant

In Fig. 5 and Fig. 6 are given the isometric section of ensemble taper bottom – support of plant and two details with section through this ensemble.



Fig. 5. The spatial section through the support and taper-bottom

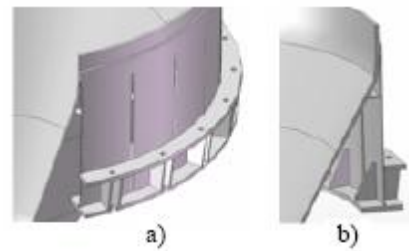


Fig. 6. The spatial details section through the support of petroleum coke plant

In Fig. 7 is given the isometric view of joint between the cylindrical body, the nervures and the shell rings of plant.

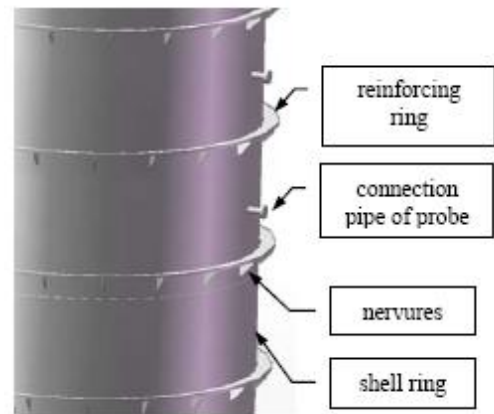


Fig. 7. A detail of joint between the reinforcing rings, nervures and shell rings

III. THE EXPERIMENTAL MEASUREMENTS

On the exterior surfaces of the reinforcing rings 1, 3, 5, 7 and 9, noted in concordance with the execution drawings, are mounted a number of 15 sensor elements in points P_1 to P_{15} placed included in planes Plane 1 and Plane 2 with scope to measure the punctual values of the velocity field which are connected to the Multilyzer analyzer, Fig. 8, [17].



Fig. 8. The position of the Multilyzer's sensors placed on the plant

The initial velocity, pressure and temperature of wind at impact with the surfaces of the metal structure, considering a constant value on whole height structure, of atmospheric front, after experimental measurements are given in Tab. 1.

Table 1. The initial v_0 , p_0 and T_0 of wind at impact

v_0 [m/s]	p_0 [Pa]	T_0 [°C]
41,66	99330	16

Also the results of measurements concerning the physical sizes in points P_1 to P_{15} are presented in Tab. 2.

Table 2. The results of measurements in points P_1 to P_{15}

Points	p [Pa]	T [°C]	ρ [kg/m ³]	v [m/s]
P ₁	99528.83	16.15	1.1981	19.251
P ₂	99739.75	16.20	1.2010	14.813
P ₃	99751.41	16.21	1.2016	14.526
P ₄	99678.42	16.20	1.2013	14.704
P ₅	99210.90	16.07	1.1970	23.405
P ₆	98254.25	16.21	1.1825	3.978
P ₇	98251.03	16.225	1.1830	2.522
P ₈	98228.03	16.226	1.1833	2.301
P ₉	98218.38	16.224	1.1837	2.936
P ₁₀	98195.43	16.196	1.1843	7.359
P ₁₁	96298.70	13.85	1.1685	69.387
P ₁₂	95743.12	13.42	1.1640	75.462
P ₁₃	95634.89	13.35	1.1636	76.438
P ₁₄	95706.18	13.44	1.1646	75.193
P ₁₅	96345.24	14.03	1.1707	66.776

IV. THE ANALYSIS WITH THE F.E.M. OF THE VELOCITY FIELD OF DYNAMICAL AIR FLOW

4.1 The initial data for numerical simulation

The study of the aerodynamically flow fields velocity around the plant with the finite element method is made with aid of the CosmosFlow 2007 software, [25].

The initial data of simulation taken into consideration:

- the variation with temperature of the air properties as the dynamical viscosity and the density, [8] and [9];
- the flow of air around the surfaces of plant including all the regimes by type laminar, by transitions and turbulent;
- the recommendation of calculus concerning the initial data of simulation give in [27];
- the incident angle of air with structure is equal with $\alpha = 90^\circ$ (situation of the maximum stress effects) and the atmospheric front which attacks the 3D plant structure has all the physical properties homogeneous, Fig. 9.

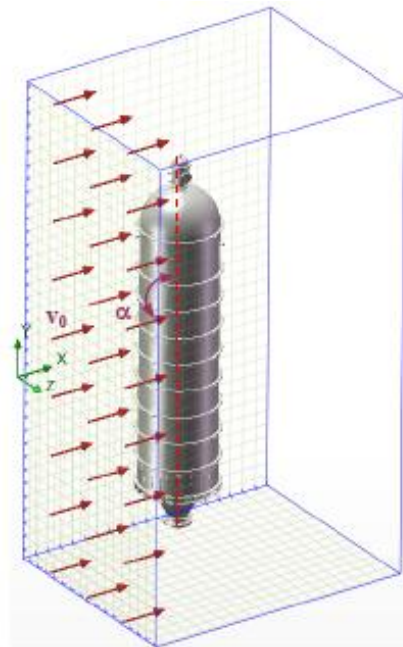


Fig. 9. The attack of the atmospheric front to the 3D structure plant

4.2. The results of simulation

4.2.1. The graphical results of simulation with the F.E.M.

In continuation are presented the 2D and 3D distribution of the velocity fields in different sections placed in horizontal or vertical planes and the distributions of the potential lines of velocity fields (the line with velocity constant property) which are accompanied by the numerical values marked on plots, Fig. 10 to Fig. 43.

The detailed specifications are given in labels attached to the presented plots.

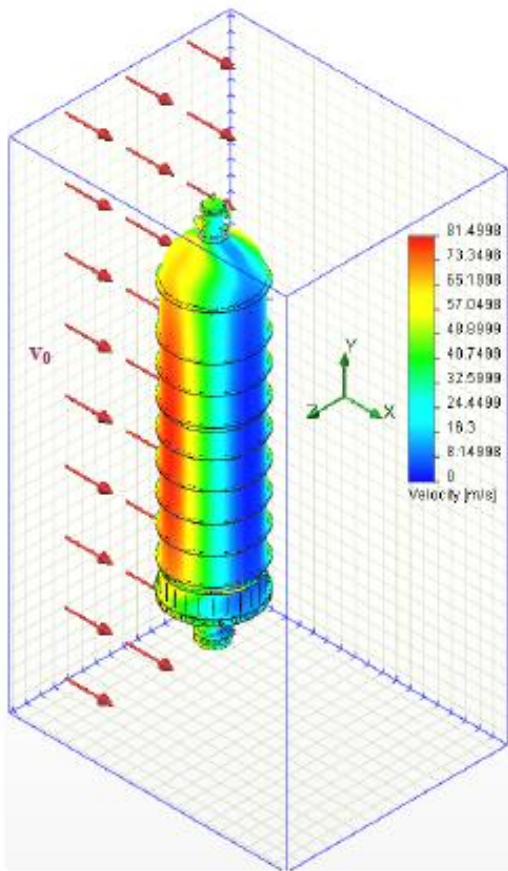


Fig. 10. The 3D velocity field on the plant's surfaces

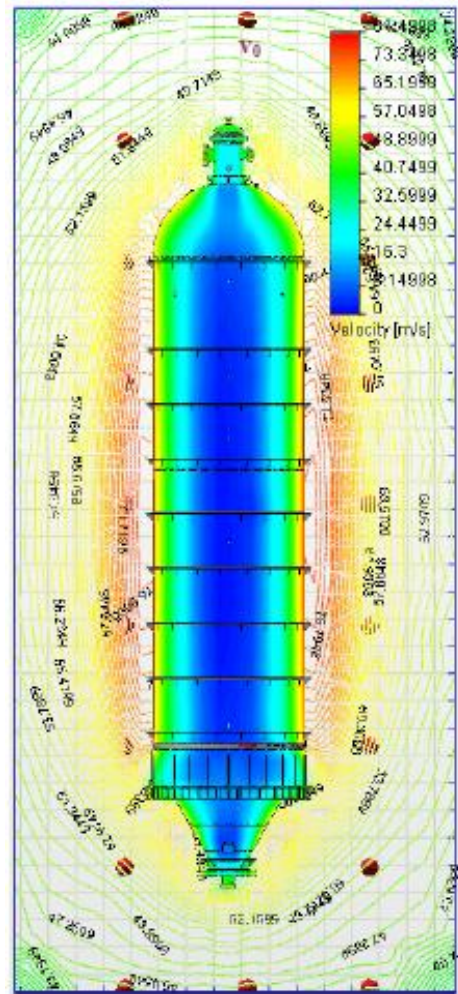


Fig. 12. The 2D potential line of velocity field on Plane 2

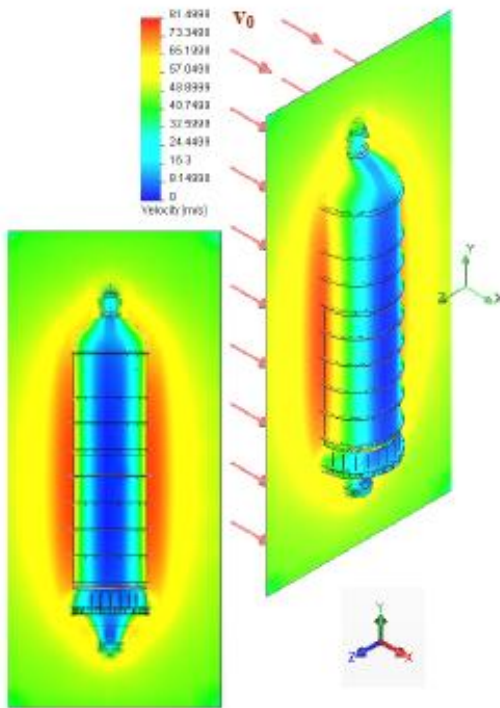


Fig. 11. The 2D velocity field on the Plane 2

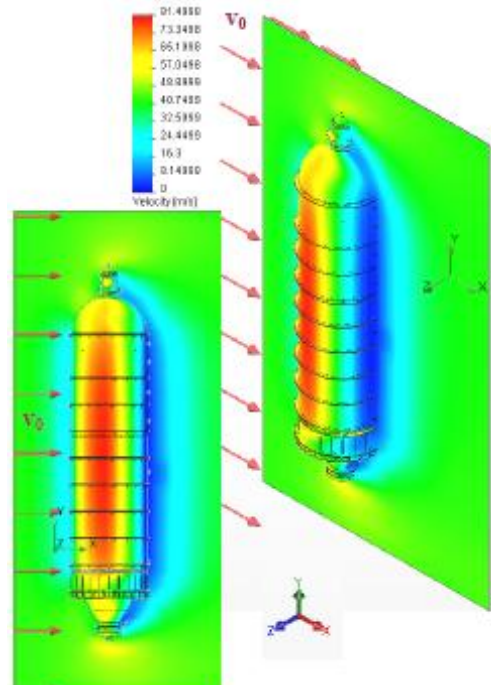


Fig. 13. The 2D velocity field on the Plane 1

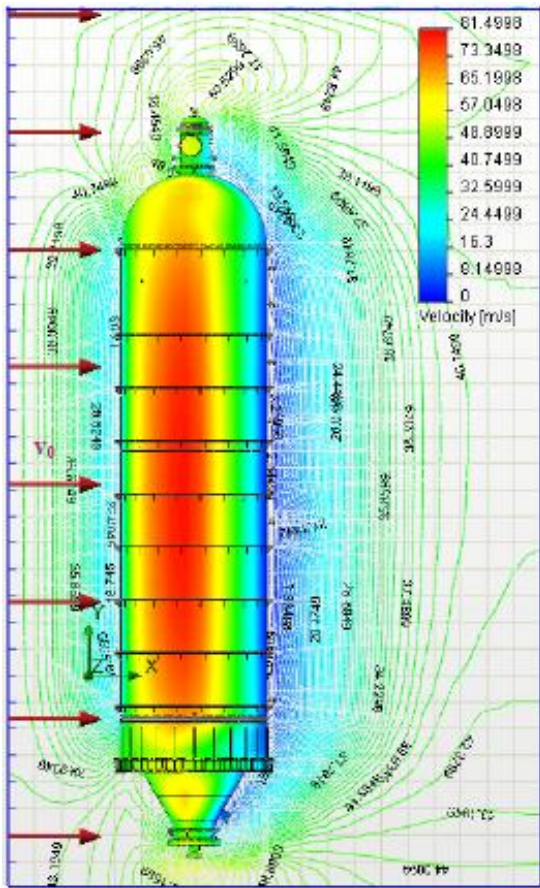


Fig. 14. The 2D potential line of velocity field on Plane 1

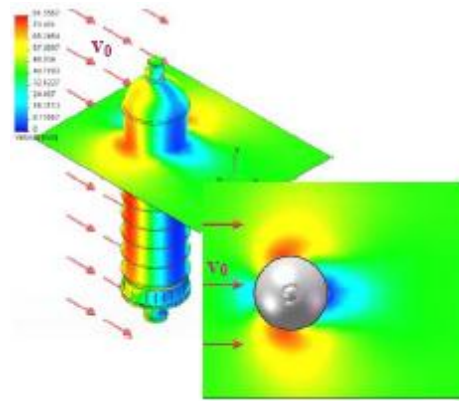


Fig. 17. The 2D velocity field on horizontal plane through the reinforcing nerve of the eighth shell ring

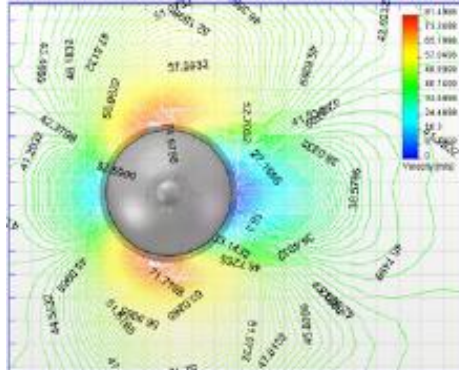


Fig. 18. The 2D potential line of velocity field on horizontal plane through the reinforcing nerve of the eighth shell ring

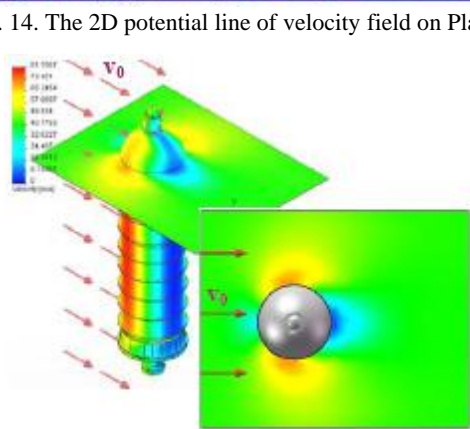


Fig. 15. The 2D velocity field on horizontal plane through the reinforcing nerve of the ninth shell ring

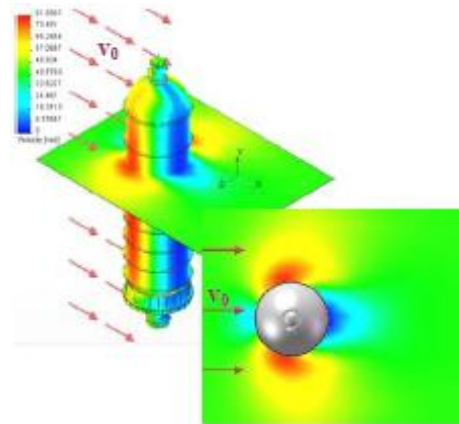


Fig. 19. The 2D velocity field on horizontal plane through the reinforcing nerve of the seventh shell ring

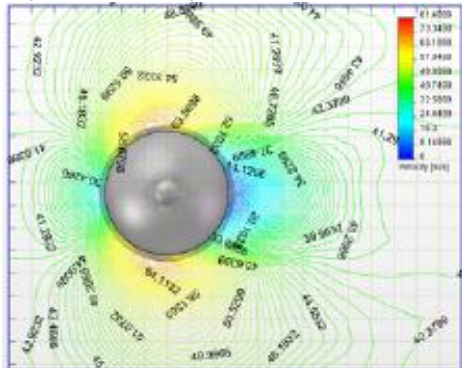


Fig. 16. The 2D potential line of velocity field on horizontal plane through the reinforcing nerve of the ninth shell ring

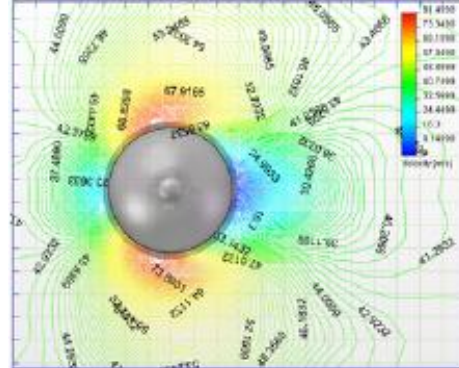


Fig. 20. The 2D potential line of velocity field on horizontal plane through the reinforcing nerve of the seventh shell ring

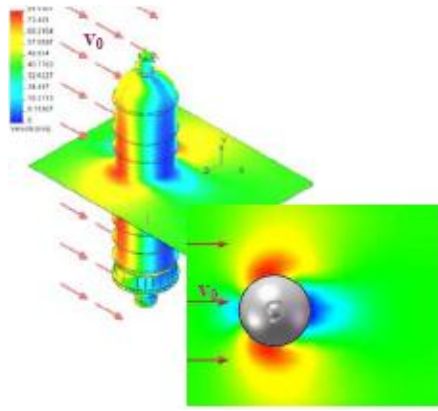


Fig. 21. The 2D velocity field on horizontal plane through the reinforcing nerve of the sixth shell ring

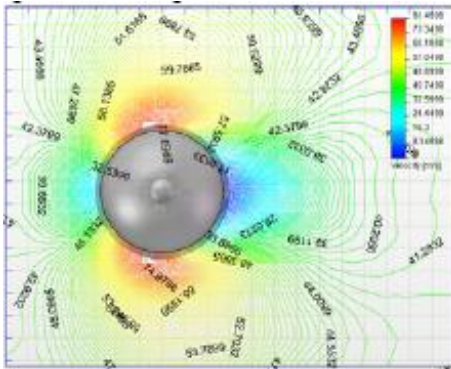


Fig. 22. The 2D potential line of velocity field on horizontal plane through the reinforcing nerve of the sixth shell ring

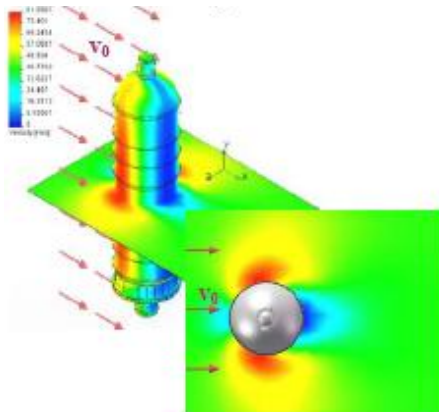


Fig. 23. The 2D velocity field on horizontal plane through the reinforcing nerve of the fifth shell ring

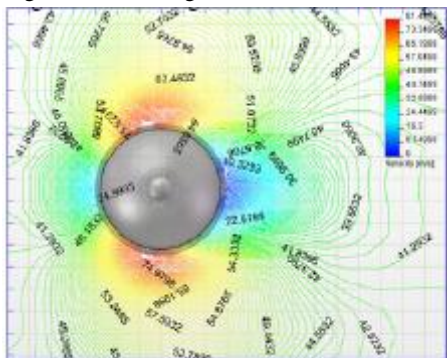


Fig. 24. The 2D potential line of velocity field on horizontal plane through the reinforcing nerve of the fifth shell ring

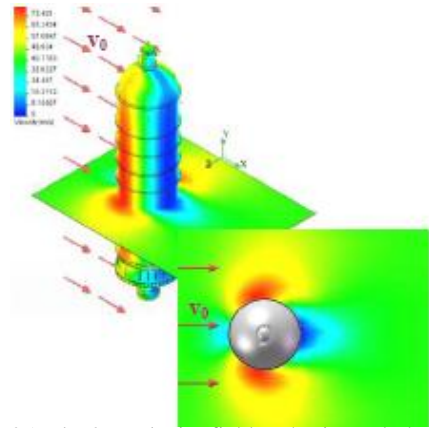


Fig. 25. The 2D velocity field on horizontal plane through the reinforcing nerve of the fourth shell ring

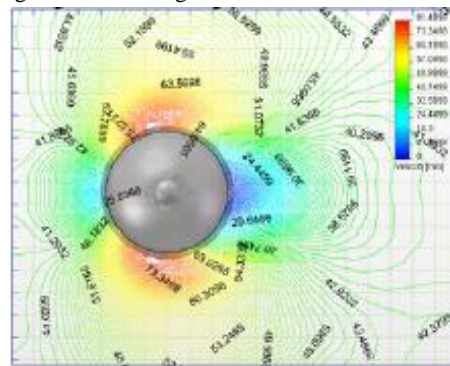


Fig. 26. The 2D potential line of velocity field on horizontal plane through the reinforcing nerve of the fourth shell ring

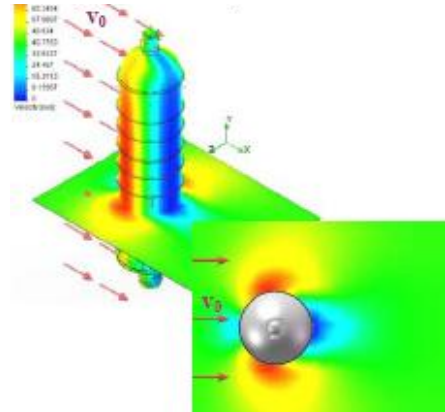


Fig. 27. The 2D velocity field on horizontal plane through the reinforcing nerve of the third shell ring

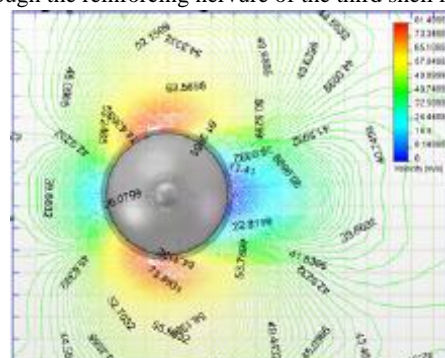


Fig. 28. The 2D potential line of velocity field on horizontal plane through the reinforcing nerve of the third shell ring

At this point is presented the velocity fields in vertical plane of section from P₁ to P₄.

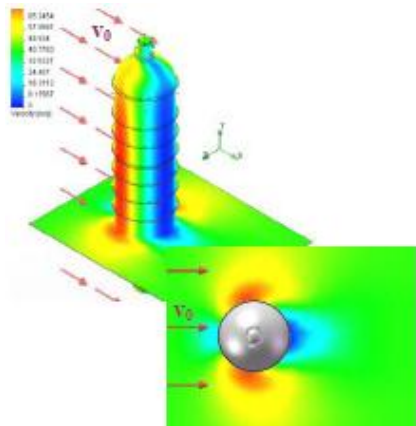


Fig. 29. The 2D velocity field on horizontal plane through the reinforcing nerve of the second shell ring

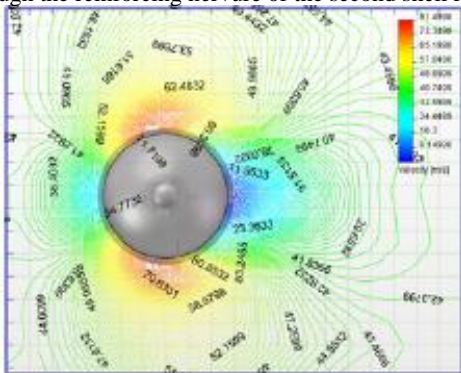


Fig. 30. The 2D potential line of velocity field on horizontal plane through the reinforcing nerve of the second shell ring

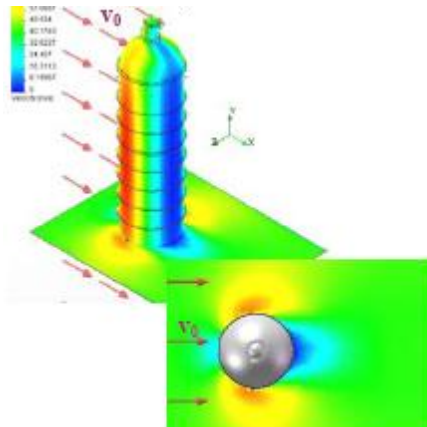


Fig. 31. The 2D velocity field on horizontal plane through the reinforcing nerve of the first shell ring

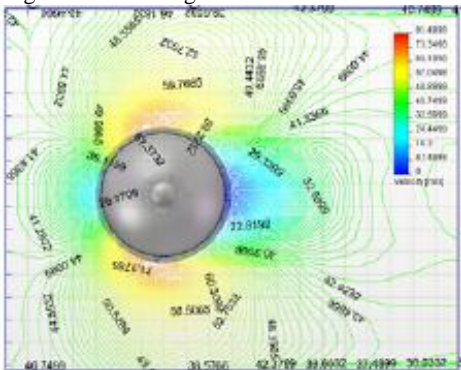


Fig. 32. The 2D potential line of velocity field on horizontal plane through the reinforcing nerve of the second shell ring

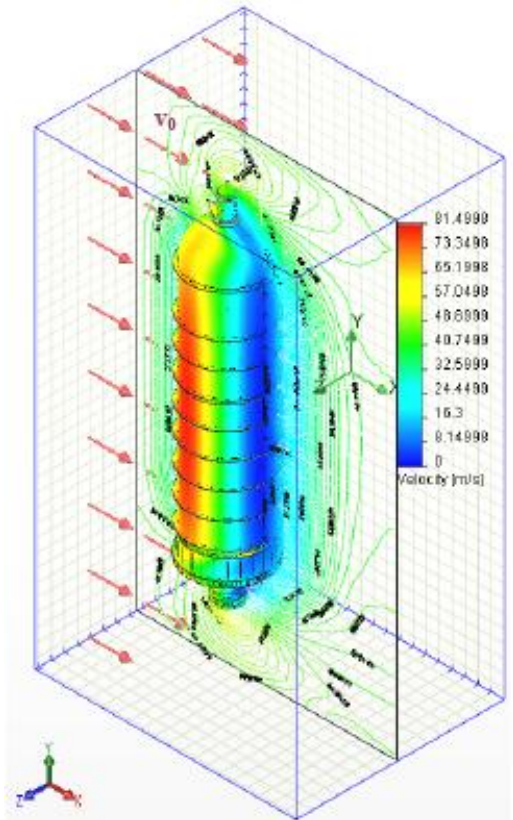


Fig. 33. The 2D potential line of velocity field on Plane 1

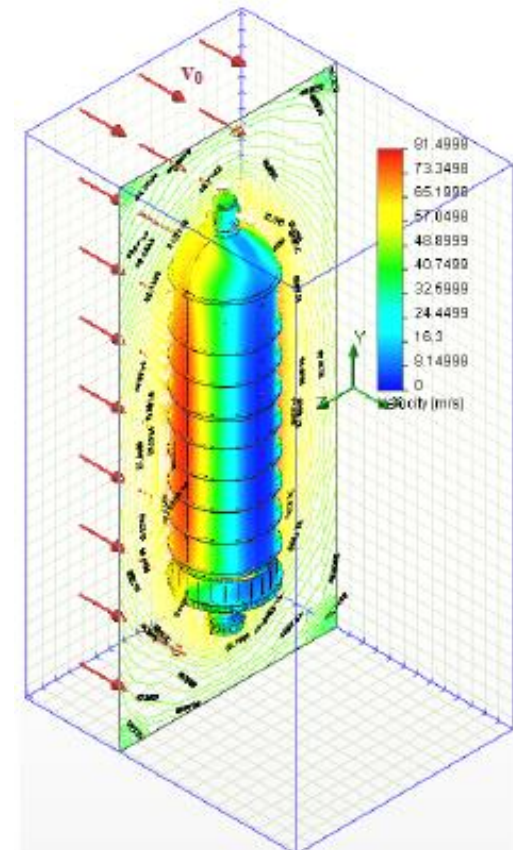


Fig. 34. The 2D potential line of velocity field on Plane 1

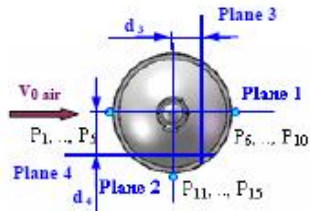


Fig. 35. The position of section on the top view of plant for vertical planes: Plane 3 and Plane 4

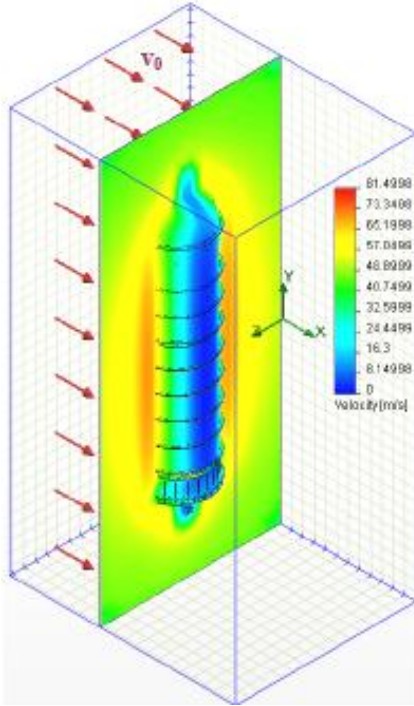


Fig. 36. The 2D velocity field on the Plane 3 corresponding to the section level at $d_3 = 1$ [m]

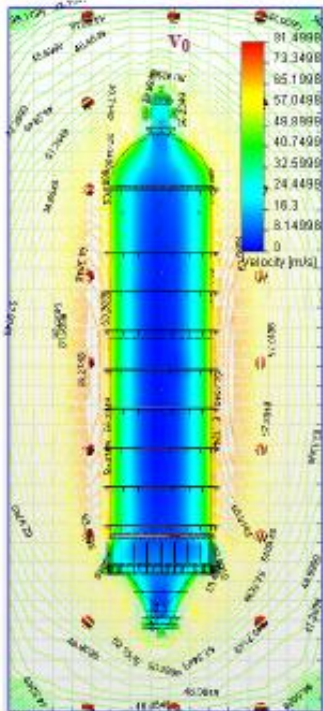


Fig. 37. The 2D potential line of velocity field on Plane 3

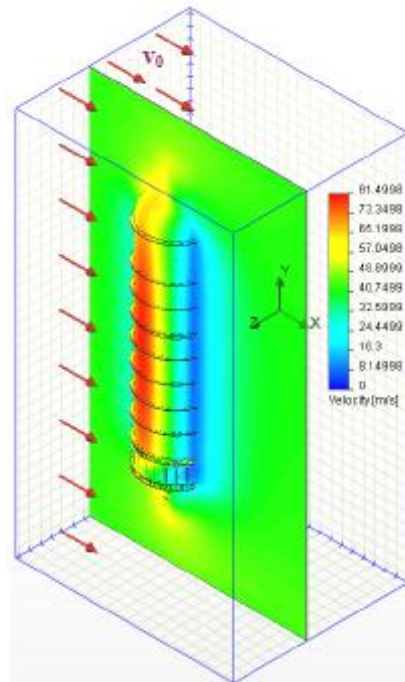


Fig. 38. The 2D velocity field on the Plane 4 corresponding to the section level at $d_4 = 1$ [m]

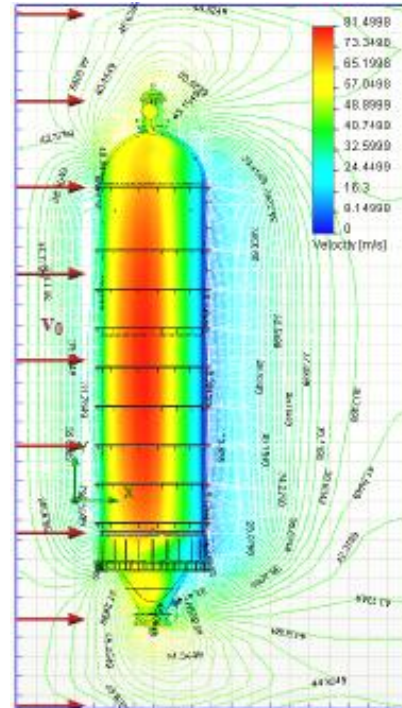


Fig. 39. The 2D potential line of velocity field on Plane 4

The character of the dynamical turbulent flow, on ensemble or in detail corresponding to the major sections of the petroleum coke plant, is presented through visualization the element fluid trajectories which are included into the velocity field (Fig. 40 to Fig. 44).

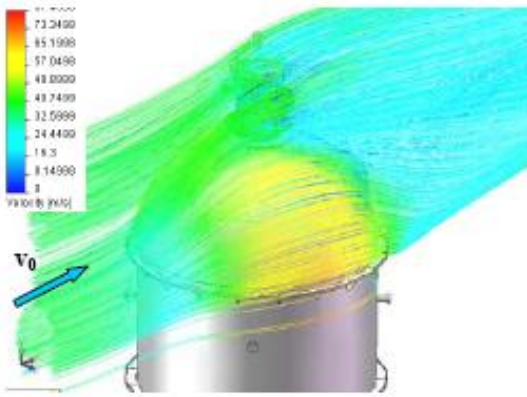


Fig. 40. The 3D trajectories flow through to the ensemble dome-spherical bottom

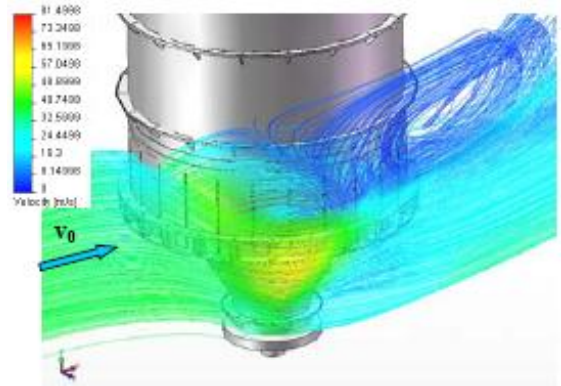


Fig. 43. The 3D trajectories flow around the taper bottom

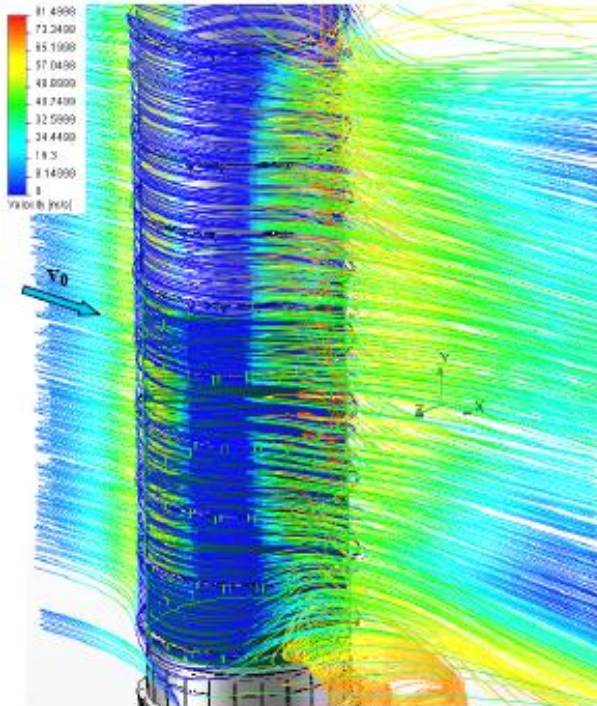


Fig. 41. The 3D trajectories flow around the cylindrical body

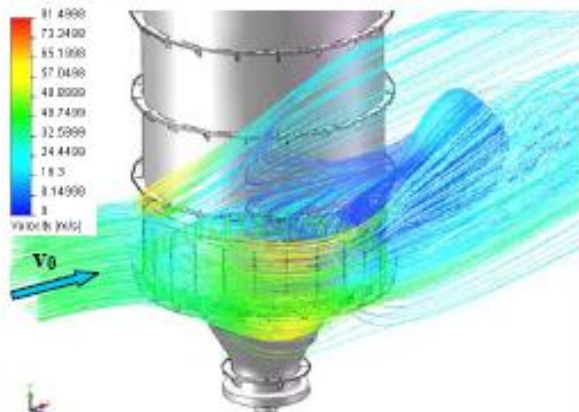


Fig. 42. The 3D trajectories flow around the support of plant

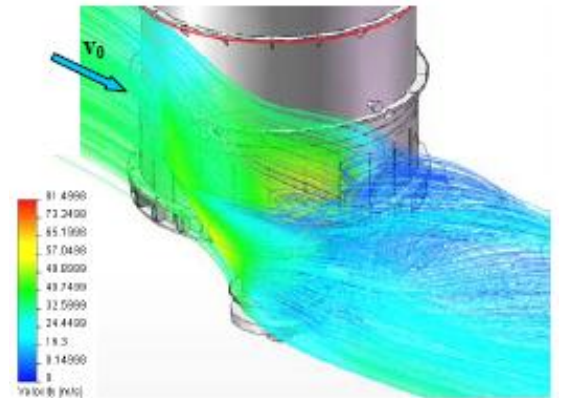


Fig. 44. The 3D trajectories flow around the taper bottom

4.2.1. The numerical results of simulation with F.E.M.

The results of numerical study made with the aid of F.E.M. concerning the values of velocity calculated in points P_1 to P_{15} and calculus of error are given in Tab. 3.

Table 3. The $v_{exp}(P_i)$, $v_{th}(P_i)$ and $\epsilon(P_i)$.

Points	v_{exp} [m/s]	v_{th} [m/s]	ϵ [%]
P_1	19.251	19.676	2.20
P_2	14.813	15.131	2.14
P_3	14.526	14.855	2.26
P_4	14.704	15.227	3.55
P_5	23.405	24.252	3.61
P_6	3.978	4.059	2.03
P_7	2.522	2.576	2.14
P_8	2.301	2.361	2.60
P_9	2.936	3.042	3.61
P_{10}	7.359	7.64	3.81
P_{11}	69.387	70.796	2.03
P_{12}	75.462	77.076	2.13
P_{13}	76.438	78.41	2.57
P_{14}	75.193	77.682	3.31
P_{15}	66.776	69.353	3.85

V. CONCLUSIONS

Analyzing the distribution fields of velocity as result of the experimental measurements and theoretical calculus (Tab. 2 and Tab. 3) we can conclude that the distributions velocity is no uniform on whole surface of petroleum coke plant.

The no uniformity fields growth up with the increasing of velocity value, Fig. 10 to Fig. 39.

The complex geometry of the external surface disturbing in totality without exceptions the distribution fields of velocity over / under or lateral of 3D metal structure of plant and the trajectories of the fluid elements are complex curves in space, Fig. 40 to Fig. 44.

The calculus of error concerning the results obtained through numerical simulations made with aid of F.E.M. is acceptable under 4 %, as result of hypothesis initial accepted that the flow of the atmospheric front have physical sizes homogeneous and the impact angle α is constant end equal with value $\alpha = 90^\circ$.

The results confirm the possibility of method to assure the precision necessary to use this method with confidence in activity of design a petroleum coke plant.

REFERENCES

- [1] Abramovici, G.N., "Teoriia turbulentnih strui", Moskva, Fizmatgiz, 1970.
- [2] Augnier R.H., "A Fast, Accurate real Gas Equation of State for Fluid Dynamic Analisis Application", *Journal of Fluids Engineering*, 1995.
- [3] Bockus S., "Solution of some differential equations of reversible and irreversible thermodynamics", *INTERNATIONAL JOURNAL OF MECHANICS*, North Atlantic University Union Publishing House, issue 1, volume 1, 2007, pp. 10-14.
- [4] Daly B.J., Harlow F.H., "Transport Equations in Turbulence". *Phys. Fluids*, 1970.
- [5] Fersiger J.H., M. Peric M., *Computational Methods for Fluid Dynamics*, Springer Verlag, 2002.
- [6] Hirsh C., "Numerical computation of Internal and External Flows. Computational Methods for Inviscid and Viscous Flows", vol. 2, JhonWiley & Sons, New York, 1984.
- [7] Hughes T.J.R., "The finite element method linear static and dynamic finite element analysis", Prentice-Hall, Inc, Englewood Cliffs, NJ, 1987.
- [8] Idelcik, I.E., "Indrumator pentru calculul rezistentelor hidraulice", Ed. Tehnica, Bucuresti, 1984.
- [9] Kiselev, P.G., "Indreptar pentru calcule hidraulice", Ed. Tehnica, Bucuresti, 1988.
- [10] Malerba M., Argento M., Salviulo A., Rossi G.L., "A boundary layer inspection on a wing profile through high resolution thermography and numerical methods", *WSEAS TRANSACTIONS on FLUID MECHANICS*, WSEAS Press, issue 1, volume 3, Jan. 2008, pp. 18-28.
- [11] Manson S.S., "Thermal stress and low-cycle fatigue", McGraw-Hill, 1974.
- [12] Marciuc G.I., "Metode de analiză numerică", Ed. Academiei R.S.R., 1983.
- [13] Patankar S.V., "Numerical Heat Transfer and Fluid Flow", Mcgraw-Hill, Washington, New-York, London, 1980.
- [14] Popescu F., Panait T., "Numerical modelling and experimental validation of a turbulent separated reattached flow", *INTERNATIONAL JOURNAL of MATHEMATICS AND COMPUTERS IN SIMULATION*, North Atlantic University Union Publishing House, issue 1, volume 1, 2007, pp. 7-11.
- [15] Reynolds A.J., "Curgeri turbulente în tehnică", Editura Tehnică, București, 1982.
- [16] Reynolds W.C., "Fundamentals of turbulences for turbulence modeling and simulation", *Lecture Notes for Von Karman Institute*, 1987.
- [17] Rizea N., "Contribuții la calculul de fluaj și oboseală al învelișurilor subțiri cu aplicație la aparatura petrochimică", Teză de doctorat, 2008, Universitatea Petrol-Gaze din Ploiești, Romania.
- [18] Sabbagh-Yazdi S.R., Mastoriakis N.E., Meysami F., "Wind flow pressure load simulation around storage tanks using SGS turbulent model", *INTERNATIONAL JOURNAL of MECHANICS*, North Atlantic University Union Publishing House, issue 2, volume 1, 2007, pp. 39-44.
- [19] Spalart P., Allmaras S., "A one-equation turbulence model for aerodynamic flow", American Institute of Aeronautics and Astronautics, 1992.
- [20] Sutton K., Gnoffo P.A., "Multi-component Diffusion with Application to Computational Aerothermodynamics", American Institute of Aeronautics and Astronautics, 1998.
- [21] Țălu M., Bolcu D., Țălu Ș., Sipos A., "The dynamic flow air visualization around the petrochemistry petroleum coke plant", *Proceedings of the 9th WSEAS International Conference on AUTOMATION and INFORMATION (ICAI '08)*, Bucharest, Romania, June 24-26, 2008, WSEAS Press, pp. 164-169. ISSN: 1790-5117, ISBN: 978-960-6766-77-0.
- [22] Țălu M., Bică M., Albotă E., Țălu Ș., "The dynamic visualization of the 3D thermal impression generated through the air friction with the petroleum coke plant structure", *Proceedings of the 5th WSEAS / IASME International Conference on ENGINEERING EDUCATION (EE '08)*, Heraklion, Greece, July 22-24, 2008, WSEAS Press, pp. 349-354, ISSN: 1790-2769, ISBN: 978-960-6766-86-2.
- [23] Țălu M., Bică M., Nanu Andrei Ghe., Albotă E., Țălu Ș., Aurelian Ș., "Visualization of dynamic behaviour of a petrochemistry petroleum coke plant under verical various seismic loadings", *Proceedings of the 10th WSEAS International Conference on Mathematical and Computational Methods in Science and Engineering (MACMESE'08)*, Bucharest, Romania, November 7-9, 2008, WSEAS Press, pp. 88-93, ISSN: 1790-2769, ISBN: 978-960-474-019-2.
- [24] **** User guide SolidWorks 2007 software.
- [25] **** User guide CosmosFlow 2007 software.
- [26] **** User guide Maple 11 software.
- [27] **** STAS 10101/2-88.